PHYSICAL REVIEW B, VOLUME 65, 014416

Scaling of hysteresis dispersion in a model spin system

J.-M. Liu*
Laboratory of Solid State Microstructures, Nanjing University, Nanjing 210093, China;
Department of Applied Physics, Hong Kong Polytechnic University, Kowloon, Hong Kong;
and Laboratory of Laser Technologies, Huazhong University of Science and Technology, Wuhan 430074, China

H. L. W. Chan and C. L. Choy
Department of Applied Physics, Hong Kong Polytechnic University, Kowloon, Hong Kong

C. K. Ong
Department of Physics, National University of Singapore, Singapore 119260
(Received 22 March 2001; published 3 December 2001)

We present a calculation of the magnetic hysteresis and its area for a model continuum spin system based on three-dimensional $(\Phi^2)^2$ model with $O(N)$ symmetry in the limit $N\rightarrow\infty$, under a time-varying magnetic field. The frequency dependence of the hysteresis area $A(f)$, namely, hysteresis dispersion, is investigated in detail, predicting a single-peak profile which grows upwards and shifts rightwards gradually with increasing field amplitude H_0. We demonstrate that the hysteresis dispersion $A(f)$ over a wide range of H_0 can be scaled by scaling function $W(\eta)\propto\tau_1 A(f,H_0)$, where $\eta=\log_{10}(f\tau_1)$ and τ_1 is the unique characteristic time for the spin reverse, as long as H_0 is not very small. The inverse characteristic time τ_1^{-1} shows a linear dependence on amplitude H_0, supported by the well-established empirical relations for ferromagnetic ferrites and ferroelectric solids. This scaling behavior suggests that the hysteresis dispersion can be uniquely described by the characteristic time for the spin reversal once the scaling function is available.

DOI: 10.1103/PhysRevB.65.014416 PACS number(s): 75.60.Ej, 75.40.Gb, 75.10.Hk

I. INTRODUCTION

When a spin system below its *Curie* point T_c is submitted to a periodic time-varying magnetic field H, say, a sinusoid field $H(t)=H_0\sin(2\pi ft)$, where t is time, H_0 is the amplitude, and f is the frequency, a looplike magnetic hysteresis is observable as plotting the system average ordering parameter (magnetization) M against field H.[1,2] It has been well established that the hysteresis is dynamic in origin,[3] i.e., the shape, symmetry, and area of the hysteresis are all f and H_0 dependent. The problem of dynamic hysteresis was not emphasized until the recent ten years. For a comprehensive review of this subject, one may refer to the article of Chakrabarti and Acharyya and references therein.[3]

In the framework of first-order phase transitions, the dynamic hysteresis is generated because of the spin-ordered domain reversal through irreversible domain wall migration (irreversible nucleation and growth), assisted by the field-induced static magnetic energy.[2] The hysteresis area A thus represents the energy dissipation (loss) in one cycle of such reversal. From a more general point of view, the hysteresis is formed due to the relaxational delay of the system responding to the external field.[3] It has been assumed that either the nucleation-and-growth mode or the relaxational delay mechanism can be described by a characteristic time that is mainly H_0 dependent. As the system responds to the time-varying external field whose characteristic time is the inverse frequency, the dynamic hysteresis is essentially determined by the two competing time scales. An understanding of the dynamic hysteresis for either real magnetic materials or model spin system is thus of interest from the point of view of basic research. On the other hand, for recording or memory applications of magnetic materials, knowledge of dynamic hysteresis enables us to understand the kinetics of domain reversal.[2] The pattern of the hysteresis and the parameters such as remanence and coercivity are essential for evaluating the materials performance. In particular, knowledge of high-frequency hysteresis is useful because high-speed spin electronics has attracted special interest nowadays.[4]

Extensive studies of the dynamic hysteresis in the past ten years have focused on two problems: the dynamic transitions and hysteresis dispersion. For the former, an increasing frequency f will break the symmetry of the hysteresis loop observed at low frequency for a given H_0, producing an asymmetric loop around the origin. The dynamic order parameter $Q=f\oint M(t)dt$, where $M(t)$ is the system average magnetization and t is time, becomes nonzero with increasing f, indicating interesting dynamic transitions in such nonequilibrium driven systems. This problem has been extensively investigated[5–9] and comprehensively reviewed.[3] Since it is irrelevant to the present work, no details will be presented here. For the latter problem, the dependence of hysteresis area A as a function of f and H_0, $A(f,H_0)$, has been studied for various magnetic systems. We present a brief review of the works along this line. The earliest work can be referred back to the well-known empirical Steinmetz law for ferrites.[10] Subsequently, the work of Rao *et al.* represents the first systematic study of the hysteresis dispersion.[11,12] They studied $O(N)$-symmetric $(\Phi^2)^2$ and $(\Phi^2)^3$ theories at $N\rightarrow\infty$ and provided a detailed analysis of the dispersion over extremely-low- and extremely-high-f ranges, respectively. It was predicted that $A(f)$ over the low- and high-f ranges exhibits the following power-law behaviors, respectively:

$$A(f,H_0) \propto H_0^{2/3} f^{1/3} \quad \text{as} \quad f \Rightarrow 0, \tag{1a}$$

$$A(f,H_0) \propto H_0^2 / f \quad \text{as} \quad f \Rightarrow \infty. \tag{1b}$$

Either following or in parallel to the work of Rao *et al.*, intensive studies on the hysteresis dispersion relationships or $A(f,H_0)$ for different systems were carried out. These include the mean-field approaches and extensive Monte Carlo simulations based on Ising-like Hamiltonians as well as experimental checking of the predicted $A(f,H_0)$ behaviors.[3] For example, Dhar and his co-workers,[13,14] Sides *et al.*,[15] and Rikvold *et al.*[16] started from the classic nucleation-and-growth concept and studied this problem in small-sized systems under small amplitude H_0. They predicted that the dispersion over an extremely-low-f range is logarithmic. However, the dispersion for the relatively high-frequency range can be better fitted with a power law, particularly when temperature T is close to the Curie point. Either when the system size is large or when H_0 is higher, the power-law behavior is followed by dispersion in a more reasonable manner. This prediction was confirmed by Monte Carlo simulations.[8,17] On the other hand, several theoretical approaches[18–21] to the dispersion overall frequency range were developed too, most of which started from solving the mean-field equation of motion for the average magnetization, predicting

$$A = A_0 + H_0^a f^b g\left(\frac{f}{H_0^c}\right), \tag{2}$$

where A_0 is the area in the $f \Rightarrow 0$ limit counting the effect from nondynamic origins, a, b, and c are the scaling exponents which take different values as reported from different sources, and g is a nonmonotonic function which meets $g(x) \Rightarrow 0$ as $x \Rightarrow 0$ or ∞. When taking the thermal fluctuations into account, Acharyya and Chakrabarti[3,8] obtained the following dispersion for $T > T_c$:

$$A(f,H_0,T) \propto H_0^a T^{-m} g\left(\frac{f}{H_0^c T^n}\right),$$

$$g\left(\tilde{f} = \frac{f}{H_0^c T^n}\right) \propto \tilde{f}^b \exp(-\tilde{f}^{\,2}/\sigma), \tag{3}$$

where m and n are scaling exponents. For $f \Rightarrow 0$, Eq. (3) reduces to a power law. The exponents depend on the system dimensionality and differ from those given in Eq. (1). Similar behavior was predicted for systems under linearly varying fields.[22]

In the meantime, several experiments on thin-film magnets,[23–26] including Co films on Cu substrates and Fe films on W(110) and Au(001) surfaces, were performed recently in order to investigate the dynamic hysteresis. Indeed, a strong dynamic contribution to the hysteresis dispersion in these systems has been demonstrated. The evaluated data on $A(f,H_0)$ can be reasonably fitted by Eq. (2), but the evaluated values for exponents a, b, and c are different from one system to another. The scattering of these data may be attributed to the difference in coercivity for these thin films, which is obviously not included in Eq. (1). A quantitative comparison of the experimentally evaluated data with the simulated exponents seems not sufficient.

Besides the works on ferromagnetic and Ising systems reported above, the problem of dynamic hysteresis in ferroelectrics is also of interest because of the high similarity between ferroelectrics and ferromagnetics in the phenomenological sense.[27] A similar mean-field approach was developed by Acharyya and Chakrabarti.[28] In addition, a phenomenological theory of the hysteresis dispersion in typical ferroelectrics, based on the nucleation-and-growth model, was proposed by Orihara and co-workers[29,30] and a power-law behavior over the low-f range was predicted. Nevertheless, for advanced ferroelectric applications, attention should be paid to the dispersion over the extremely-high-f range, which remains challenging to us.

From all of the above description, we understand that the physical mechanism underlying the dynamic hysteresis is the competition of the two time scales. Although it is well accepted that the dynamic response at any fixed H_0 exhibits some characteristic time scale, the uniqueness of this time scale remains to be identified. From the general point of view, the evolution of some physical quantity associated with the system order parameter, no matter whether it is conserved or not, may be scaled by a generalized scaling function.[2,31] Such a scaling behavior predicts the existence of a unique characteristic parameter to describe the evolution. In this paper, we study the scalability of the hysteresis dispersion. Let us discuss the magnetic hysteresis under a time-varying magnetic field from the point of view of the nucleation-and-growth concept. It is believed that spin reversal contributes dominantly to hysteresis generation, unless f is extremely high (typically 10^7 Hz for ferrites). A direct argument is that the dispersion $A(f)$ under different H_0 should be scalable if a unique characteristic time τ_1 for the spin reversal is available and no other mechanism besides the spin reversal contributes to the hysteresis. This picture is physically quite similar to the dynamic scaling in diffusion-limited precipitation in supersaturated systems in which the correlation length of the second phase is a unique characteristic quantity.[31] Therefore, if there exists a one-variable scaling applicable to the hysteresis dispersion, the characteristic time scale for the system response should be unique.

The present paper focuses on the scaling behavior in spin systems. We calculate the dispersion relation for the model continuum spin system based on the three-dimensional $(\Phi^2)^2$ model with $O(N)$ symmetry. Our results demonstrate the scalability of the hysteresis dispersion in this system. The remaining part of this paper is organized as follows: in Sec. II we introduce the model continuum spin system and the numerical algorithm. The calculated dispersion and proposed scaling analysis will be presented in Sec. III, together with a discussion of the experimental relevance. A brief conclusion is given in Sec. IV.

II. MODEL AND NUMERICAL CALCULATION

We start from the N-component $(\Phi^2)^2$ model with $O(N)$ symmetry in three dimensions as responding to field H

$=H_0 \sin(2\pi ft)$. Although this model was introduced previously,[11] a brief description is presented here for clarification. Because the magnetization is not conserved, its relaxation in due course is described by the nonconserved order parameter dynamics. This model is exact in the limit $N \to \infty$. The evolution of the system order parameter set Φ obeys the Langevin equation

$$\frac{\partial \Phi_\alpha}{\partial t} = -\Gamma \frac{\delta F}{\delta \Phi_\alpha} + \eta_\alpha, \tag{4}$$

with the Gaussian white noise η_α:

$$\langle \eta_\alpha(x,t) \rangle = 0,$$

$$\langle \eta_\alpha(x,t)\, \eta_\beta(x',t') \rangle = 2\Gamma \delta_{\alpha\beta} \delta(x-x')\, \delta(t-t'), \tag{5}$$

where $\alpha, \beta = 1,2, \ldots, N$, represent the orientation in the spin space, respectively; x is the spatial coordinate, Γ is the mobility for the spin-lattice relaxation ($\sim 10^7$ Hz for ferrites), and F is the free-energy function [$(\Phi^2)^2$ type],

$$F = \int d^3x \left[\frac{1}{2} J \langle \nabla \Phi_\alpha)(\nabla \Phi_\alpha) + \frac{r}{2}(\Phi_\alpha \Phi_\alpha) + \frac{u}{4N}(\Phi_\alpha \Phi_\alpha)^2 - \sqrt{N} H_\alpha \Phi_\alpha \right], \tag{6}$$

where Φ is an N-component vector and J is the interaction between two components; $r = T - T_c^{TF}$ where T_c^{TF} is the mean field T_c with $T_c < T_c^{TF}$ in the general case; u is the prefactor and counts the contribution of the second-order nonlinear interaction, and $u = -2\pi^2 (T_c - T_c^{TF})$. Since $\Phi_\alpha \Phi_\alpha$ scales as N, each term in the bracket scales as N, and therefore so does the free energy. We assume the external field $H_\alpha = H \delta_{\alpha,1}$, pointing to axis $\alpha = 1$. Equation (4) is equivalent to an infinite hierarchy of differential equations for the cumulants of Φ_α. In the $N \to \infty$ limit, this infinite hierarchy of differential equations is truncated and the following coupled integrodifferential equations are obtained:[11,32]

$$\frac{dM(t)}{dt} = \frac{1}{2}[M(t)K(t) + H_0 \sin(2\pi ft)],$$

$$K(t) = -[r + uM^2(t) + uS(t)],$$

$$S(t) = \frac{1}{2\pi^2} \int_0^1 q^2 C_T(q,t)\, dq,$$

$$\frac{dC_T(q,t)}{dt} = -[q^2 - K(t)] C_T(q,t) + 1, \tag{7}$$

where $M(t)$ is the component of the order parameter **M** along spin direction $\alpha = 1$, i.e., magnetization, and $C(q,t)$ is the correlation function which has the transverse component $C_T(q,t)$ ($\alpha \neq 1$) and longitudinal component $C_L(q,t)$ ($\alpha = 1$):

$$M(t) = \langle \Phi_1(q,t) \rangle,$$

$$C_T(q,t) = \langle \Phi_\alpha(q,t) \Phi_\alpha(-q,t) \rangle, \quad \alpha \neq 1,$$

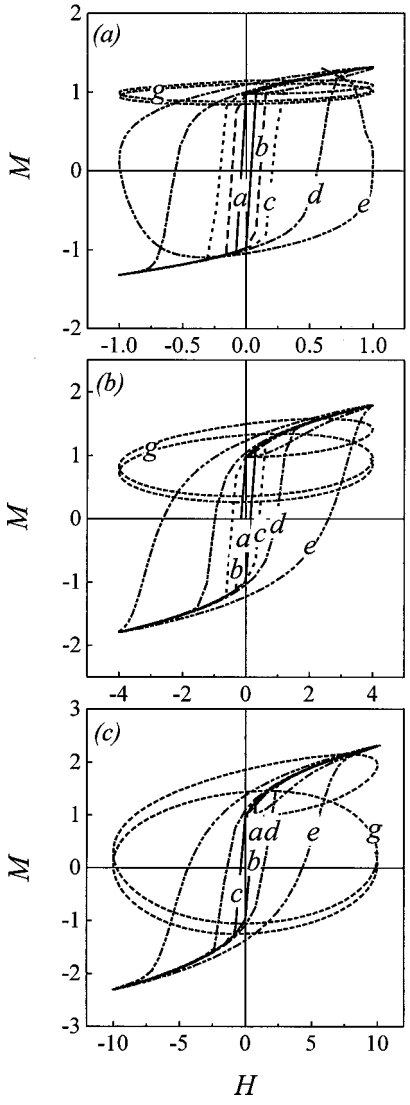

FIG. 1. Hysteresis loops as calculated at different frequencies and amplitudes, $r = -0.1$ and $u = 1.0$. *a*: $f = 1.5 \times 10^{-5}$. *b*: $f = 1.0 \times 10^{-4}$. *c*: $f = 6.0 \times 10^{-4}$. *d*: $f = 6.0 \times 10^{-3}$. *e*: $f = 0.06$. *g*: $f = 0.6$.

$$C_L(q,t) = \langle \Phi_1(q,t) \Phi_1(-q,t) \rangle. \tag{8}$$

The numerical procedure for the hysteresis given by Rao *et al.*[11] is utilized in our calculation in which various values for r and u are taken. The time step Δt as a replacement of dt is 10^{-7} with a unit of $(2\Gamma)^{-1}$ at low f ($\sim 10^{-5}$) and reduced with increasing f, until a further reduction of Δt does not produce any variation of the output data within our numerical uncertainty.

III. RESULTS AND SCALING ANALYSIS

A. Shape evolution of hysteresis

The hysteresis loops as r and u take different values are evaluated. Figures 1(a)–1(c) present the calculated hysteresis at different H_0, respectively, as $r = -1.0$ and $u = 1.0$. For each given H_0 six loops obtained at different frequencies

covering $10^{-5}-10^{0}$ are plotted. A considerable dependence on f of the hysteresis in shape and area is clearly revealed. Take Fig. 1(a) where $H_0=1.0$ as an example. The loops are well saturated and show thin squarish shape as f is low. With increasing f, the loop expands along the H_0 axis, producing increasing coercivity. The high-field magnetization remains saturated. The loops show fat squarish or rhombic pattern. With further increase in f, the loop has no longer saturated M at maximum field and a corner-rounded elliptical pattern is observed. At this stage the loop still remains symmetric around the origin. At an even higher f, the loop becomes asymmetric around the origin and a positive bias appears. At an extremely high f, the calculation produces no more loop-like hysteresis, but only a slightly tilted line.

Such a pattern evolution of the hysteresis is repeated as H_0 takes higher values [$H_0=4.0$ in Fig. 1(b) and $H_0=10.0$ in Fig. 1(c)], while the transition from one shape to another appears at a higher f. For instance, for the same value of f (loop e), the hysteresis in Fig. 1(a) is a seriously asymmetric one, but it becomes symmetric in Fig. 1(b) until a well-defined and saturated one in Fig. 1(c). Furthermore, the evolution sequence remains quite similar as the temperature parameter r is different. In fact, at a lower temperature (more negative r) one just sees higher coercivity and remanence as well as a more squarish shape. A detailed description of this evolution and related stability diagram has been given previously.[11]

Such evolution of hysteresis with increasing frequency can be qualitatively explained in terms of spin-reversal kinetics. Keeping in mind the simple assumption that the kinetics of spin reversal can be characterized by a characteristic time, say, τ, one understands that the shape and area of the hysteresis are fully determined by the relative dominance between τ and f^{-1}. Surely, the results shown in Fig. 1 tell us that this characteristic time depends on H_0. If $\tau \ll f^{-1}$, the spin reversal in the system can be sufficient, resulting in near-equilibrium (quasistatic) hysteresis. As $\tau \gg f^{-1}$, the spin reversal cannot catch up in kinetics with the field oscillation such that an unsaturated elliptical loop or even geometrically nonconverged loop is generated.

B. Hysteresis dispersion

If the above argument on the characteristic time is true, the hysteresis dispersion must exhibit a single-peaked pattern. The calculated hysteresis dispersion $A(f)$ at various H_0 is presented in Fig. 2 for $r=-1.0$ and $u=1.0$ and in Fig. 3 for $r=-3.0$ and $u=1.0$, respectively, in which the f axis is in a logarithmic scale. It is clearly indicated that $A(f)$ indeed exhibits the single-peak pattern which is slightly tilted towards the high-frequency side. What should be mentioned here is that a preevaluation by taking much more data dots does not show any tail of the second peak if any. As H_0 increases, the peak position shifts gradually rightwards the high-f side and the peak value increases too. Furthermore, all curves remain similar in shape from one to another, thus predicting the possibility of one-parameter scaling.

Comparing the calculated data at different temperatures, $r=-1.0$ and -3.0, allows us to conclude that the dispersion

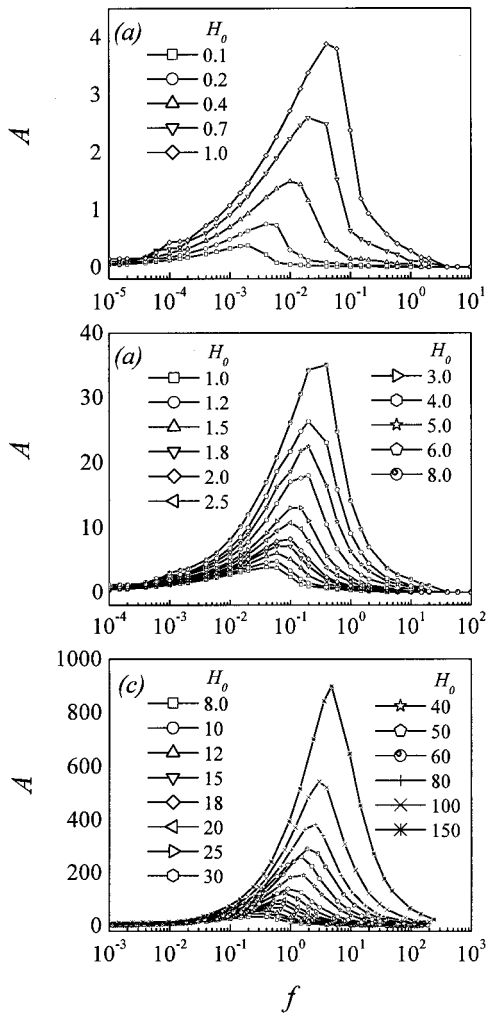

FIG. 2. Hysteresis dispersion $A(f)$ under various H_0 as labeled at $r=-1.0$ and $u=1.0$.

behavior remains the same and no qualitatively identifiable difference between them can be found. A careful comparison advises us that given a value of H_0 the dispersion curve shows a lower peak value but a higher-f position as the temperature is higher (r is bigger). This is understandable because a shorter characteristic time τ and a lower coercivity are expected at a higher temperature, while the magnetization is lower too.

In addition, the field-dependence analysis allows us to conclude that the hysteresis dispersion indeed shows power-law behaviors over the low- and high-f ranges, well consistent with Eq. (1). While the results remain the same as those reported previously,[11] no more detailed description on the power-law behaviors will be given here. We shall come back to this point in Sec. III E.

C. Scaling analysis

In order to check the existence of a characteristic time τ applicable to spin reversal, we perform the one-variable scaling analysis.[33] To evaluate an arbitrary nth scaling momentum of the dispersion, i.e., $S_n=\int_0^\infty f^n A(f)df$, the high-

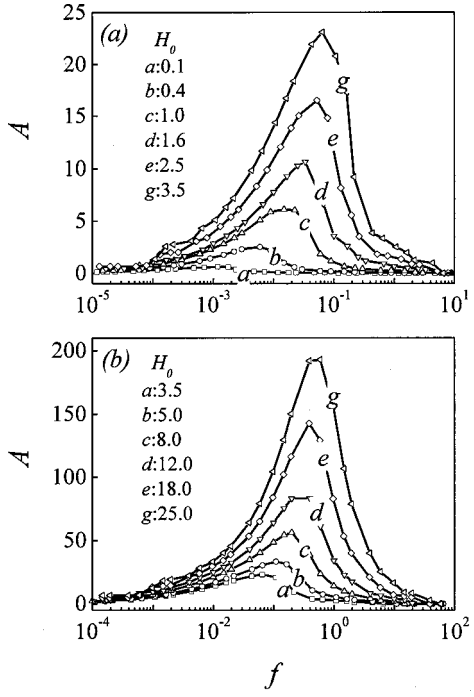

FIG. 3. Hysteresis dispersion $A(f)$ under various H_0 as labeled at $r=-3.0$ and $u=1.0$.

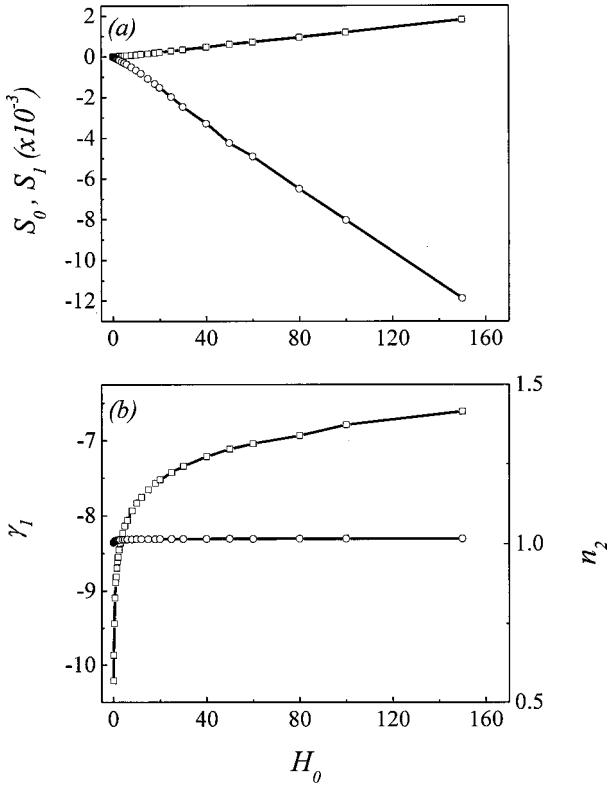

FIG. 4. Scaling variables S_n, γ_1, and n_2 as a function of amplitude H_0 at $r=-1.0$ and $u=1.0$.

frequency decaying of $A(f)$ must be faster than the term $f^{(n+1)}$. Referring to Eq. (1b), we understand that the *zeroth* momentum S_0 is already diverse. A modified definition of the scaling parameter such as S_n is thus required. In fact, it is more reliable to replace variable f with $\log_{10}(f)$. One may define several scaling parameters:

$$\gamma=\log_{10}(f\tau_0)$$

$$S_n(H_0)=\int_{-\infty}^{\infty}\gamma^n A(\gamma,H_0)d\gamma, \quad n=0,1,2,\ldots,$$

$$\gamma_n(H_0)=S_n(H_0)/S_0(H_0),$$

$$n_2(H_0)=S_2(H_0)/S_1^2(H_0), \tag{9}$$

where τ_0 is a time constant chosen arbitrarily (10^{-7} used here), γ is the modified frequency, S_n is the nth momentum as defined above, γ_n is the nth characteristic frequency, and n_2 is the scaling factor. Note here that for the high-f range, one has $A(f)\propto f^{-1}\propto 10^{-\gamma}$ so that the integral $\int_0^{\infty}\gamma^n A(\gamma)d\gamma$ is always converged as long as n is finite. For the low-f range, one has, from Eq. (1a), $A(f)\propto f^{1/3}\propto 10^{\gamma/3}$. The integral $\int_{-\infty}^{0}\gamma^n\times 10^{\gamma/3}d\gamma$ also converges to a finite value, no matter how big the integer n is. Therefore, the scaling parameters as given in Eq. (9) are mathematically definable.

When our data over $f=10^{-6}-10^{2}$ in place of $0<f<\infty$ are used for evaluating the above parameters, the as-produced uncertainties are less than 0.01. These parameters as a function of H_0 each are plotted in Fig. 4 for $r=-1.0$ and $u=1.0$. Apart from the cases where H_0 is very small ($H_0<1.0$), a perfectly linear $S_n(H_0)$ is obtained. The parameter γ_1 shows a gradual growth with increasing H_0, but the scaling factor n_2 remains unchanged within the calculation uncertainty. For other temperatures, the same conclusion is obtained. The independence of n_2 on H_0 over a wide range of H_0 indicates that the dispersion curves at different H_0 can be scaled using a one-parameter scaling function.

To construct such a scaling function, one assumes that a unique characteristic time for spin reversal exists, which scales the kinetics of spin reversal at a given H_0. If the scaling behavior is approved, this assumption becomes true. Because the time scale is definable only in one-dimensional space, i.e., the possible exponent for time is 1, the scaling function can be constructed by multiplying the characteristic time by the hysteresis dispersion. The scaling function may take the following form:

$$W(\eta)=\tau_1/\tau_0 A(\gamma,H_0), \tag{10}$$

with

$$\eta=\log_{10}(f\times\tau_1),$$

$$\log_{10}(\tau_0/\tau_1)=\gamma_1,$$

$$\tau_1=\tau_0\times 10^{-\gamma_1}, \tag{11}$$

being the scaling variables (i.e., scaled frequency) and the effective characteristic time for the spin reversal. Correspondingly, we can define the effective characteristic frequency $f_1=\tau_0/\tau_1$, so that Eq. (10) can be rewritten as

$$W(\eta)=f_1^{-1}A(\gamma,H_0). \tag{12}$$

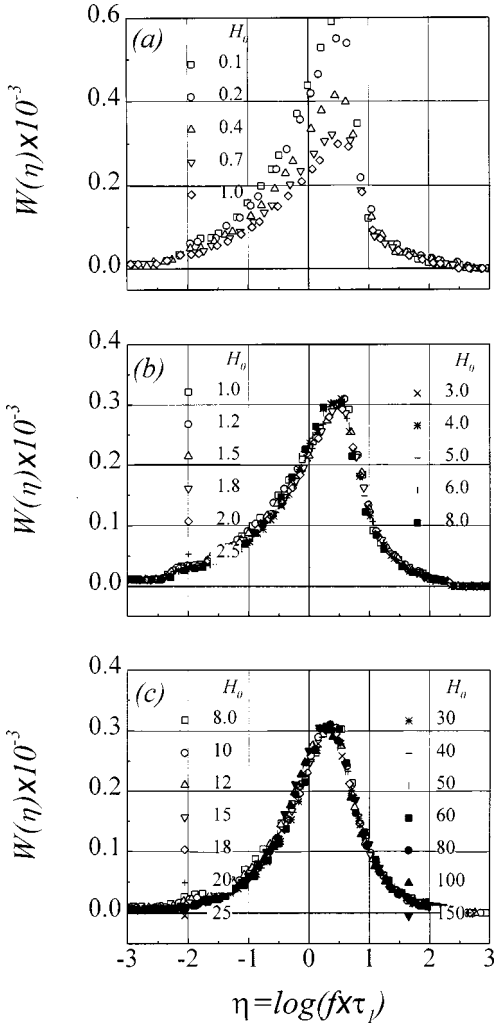

FIG. 5. Scaling function $W(\eta)$ as evaluated by scaling transform, Eq. (8), applied to all hysteresis dispersion curves $A(f)$. Here $r=-1.0$ and $u=1.0$.

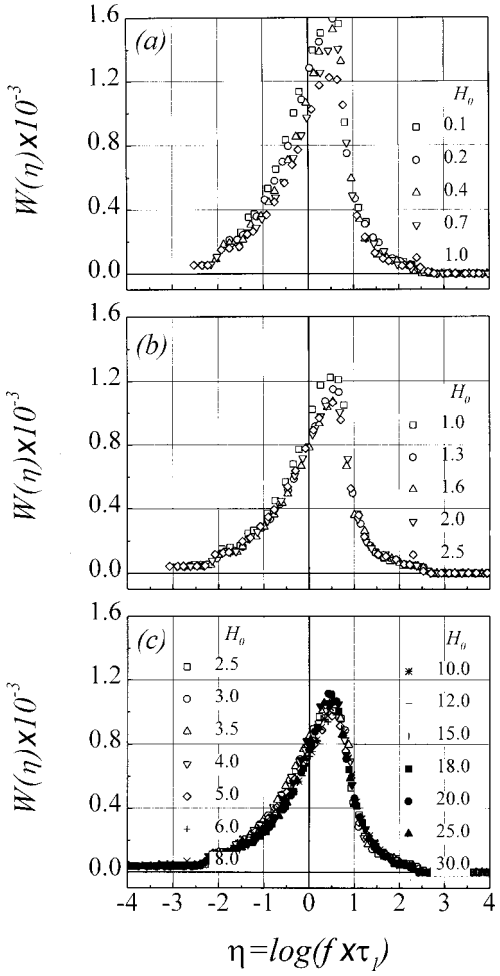

FIG. 6. Scaling function $W(\eta)$ as evaluated by scaling transform, Eq. (8), applied to all hysteresis dispersion curves $A(f)$. Here $r=-3.0$ and $u=1.0$.

Plotting all calculated dispersion curves $A(f)$ after transforming them according to Eqs. (10) and (11) produces Figs. 5 and 6 for $r=-1.0$ and -3.0 and $u=1.0$, respectively. It is clearly shown that apart from the cases where H_0 is very small (typically $H_0<1.0$), all dispersion curves $A(f)$ fall onto the same curve within the numerical uncertainties, demonstrating the scaling property of the hysteresis dispersion. This indicates that for spin reversal in the model continuum spin system, there indeed exists a unique characteristic time which is either τ_1 or a time proportional to τ_1, by which the hysteresis dispersion effect can be uniquely characterized.

It is interesting to compare this scaling behavior for the hysteresis dispersion with the scaling for the diffusion-limited precipitation (DLP).[2,31] For the latter, one understands that the structure function $S(q,t)$, where q is the spatial wave vector for the system, also shows the single-peaked pattern and is proportional to the spatial correlation between the compositional variable. $S(q,t)$ at different t can be scaled using the scaling transform

$$W(q/q_1)=q_1^3 S(q,t), \tag{13}$$

where q_1 is the characteristic wave vector to uniquely scale the time evolution of the structure function. Here the exponent for wave vector q_1 is 3 because q_1 is defined in three-dimensional space. A surprising similarity between Eqs. (12) and (13) is shown. At the same time, the DLP problem can be described by a Langevin equation similar to Eq. (4) with similar order parameter of nonconservation.[2]

Our calculation confirms too that scaling function, Eq. (10), applies over a wide range of temperature r. The only difference lies in the magnitude of function $W(\eta)$.

D. Field dependence of time τ_1

Let us look at the characteristic time τ_1 as a function of H_0, as presented in Fig. 7 in a double-logarithmic scale. The solid line represents an inversely linear relationship between τ_1 and H_0: i.e., the exponent for f_1 is 1:

$$\tau_1 \propto H_0^{-1},$$

$$f_1 \propto H_0. \tag{14}$$

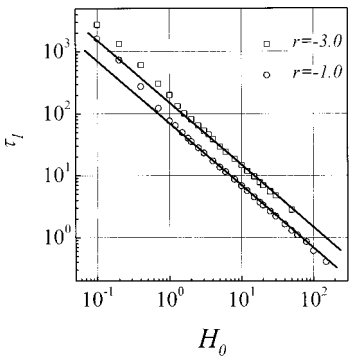

FIG. 7. Characteristic time τ_1 for the spin reversal as a function of amplitude H_0. Here $u=1.0$.

Our data at two temperatures reveal clearly that the characteristic time τ_1 is linearly dependent of H_0 as long as H_0 is not very small. In the other words, the relationship between τ_1 and H_0 becomes linear once the dispersion reaches the scaling state or vice verse. When $H_0 \leqslant 1.0$, a superficial deviation of the data from the linear relation is observed, an explanation of which will be given below. Equation (14) predicts that τ_1 is shorter and f_1 is higher if H_0 is higher. As for the temperature dependence, a shorter τ_1 for a higher temperature is indicated in Fig. 7, a well-accepted conclusion.

The unity exponent as defined in Eq. (14) is general for scaling phenomena for the first-order phase transitions. For the DLP phenomena mentioned above, the same exponent applies if correlating q_1 and time for the evolution of $S(q,t)$:

$$q_1^3 \propto t^{-1}, \tag{15}$$

which has been well evidenced, as long as t is not very small.[34]

E. Power-law behaviors of the scaling function

It is of interest to check the frequency dependence of the scaling function over the low- and high-f ranges, respectively. In fact, we see clearly that the power-law behaviors for the hysteresis dispersions, as predicted in Eq. (1), remain unaffected by the scaling transform, Eq. (10). We rewrite Eq. (1) as

$$W(f\times\tau_1) \propto (f\times\tau_1)^{1/3} \quad \text{as} \quad f \Rightarrow 0, \tag{16a}$$

$$W(f\times\tau_1) \propto (f\times\tau_1)^{-1} \quad \text{as} \quad f \Rightarrow \infty. \tag{16b}$$

As an example, we present in Fig. 8 all rescaled dispersions $W(f\times\tau_1)$ at different H_0 as a function of $f\times\tau_1$ and a linear behavior over the low-f range is shown for each case. The power law, Eq. (16a), is confirmed. The same is applicable to Eq. (16b).

What should be mentioned here is that Eqs. (16) are actually another form of Eqs. (1). Substituting Eqs. (12) and (14) into Eqs. (16), we obtain Eqs. (1) once more.

F. Experimental relevance

Up to date there have been no sufficient data for ferromagnetic solids to check the scalability of the hysteresis dispersions. We consider the linear relationship between τ_1 and H_0, Eq. (14), as derived from the scaling analysis. Equation (14) is not a new theoretical prediction. For ferrite solids, typical ferromagnetics, it was experimentally reported 30 years ago that the following empirical relationship holds if spin reversal takes place predominantly as a result of irreversible domain wall migration:[10]

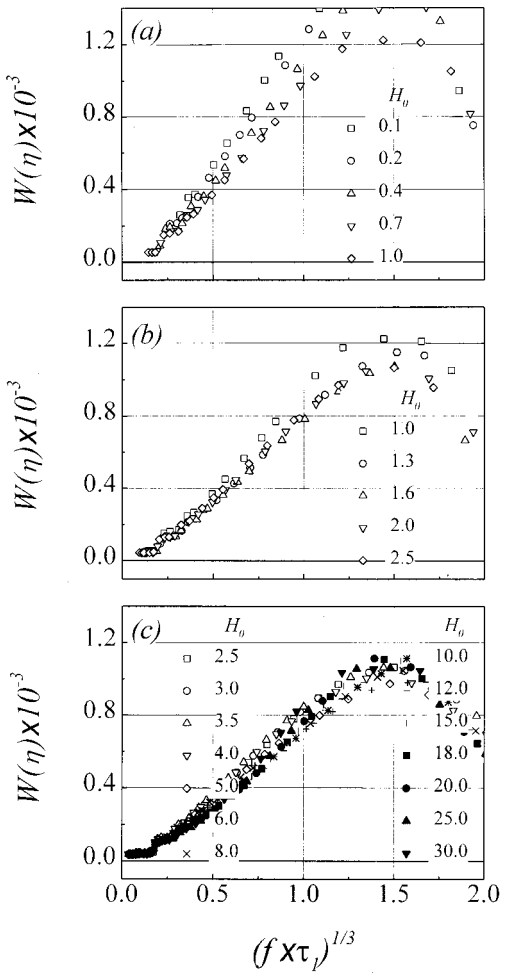

FIG. 8. Power-law dependence of scaling function W on frequency $f\times\tau_1$ over the low-f range, with an exponent of 1/3. Here $r=-3.0$ and $u=1.0$.

$$(H_0 - H_f)\tau' = \text{const}, \tag{17}$$

where H_f is a constant slightly smaller than the stationary coercivity and τ' is the time defined as that for a half-reversal of the magnetization, i.e., some characteristic time for spin reversal. Since H_f is quite small compared to H_0, unless the latter is so low that no regular hysteresis is obtained (no irreversible spin reversal occurs), Eq. (17) is equivalent to Eq. (12). Also, as H_0 is very close to H_f, τ' has to be bigger than the prediction from the linear relationship $H_0\tau' = \text{const}$. Therefore, this empirical relation explains the superficial deviation of the data from the straight lines, as shown in Fig. 7.

Nevertheless, it should be pointed out that as $H_0 < H_f$, the fast and reversible domain rotation rather than irreversible

domain wall motion is responsible for the hysteresis generation. Such a fast domain rotation is highly related to thermal fluctuation-activated spin switching, which is reversible and thus very rapid. Consequently, a negative deviation of the characteristic time from the inversely linear relationship, Eq. (14), is possible. Unfortunately, reversible spin switching at $H_0 < H_f$ seems not reachable by the present model.

On the other hand, we may consider similar empirical relations established for typical ferroelectric oxides such as $BaTiO_3$ (BTO) and $KNbO_3$ (KNO), although the present continuum model as applied to ferroelectric polar systems does not predict any ferroelectric transition.[35] However, the domain reversal through irreversible domain boundary motion in ferroelectric solids remains similar to that in ferromagnetic ones. We consider the case in which both multinucleation and domain boundary motion occur concurrently.[36] Once the applied electric field is not very low, the new domain nucleation rate in BTO can be expressed as $p(1/ms) \propto E_0^{2/3}$, where E_0 is the field magnitude, so that a characteristic time $\tau_n \propto E_0^{-2/3}$ can be obtained. Furthermore, the domain boundary motion velocity as a function of E_0 takes the form $\nu \propto E_0^{4/3}$, from which a second characteristic time $\tau_\nu \propto E_0^{-4/3}$ is predicted. The domain reversal can thus be characterized by an effective time

$$\tau' = \sqrt{\tau_n \tau_\nu} \propto E_0^{-1}, \tag{18}$$

which as a function of E_0 takes the same form as Eq. (12). Note that there were no high-f data available to confirm this relation. For KNO, the measured domain switching time as a function of E_0 was reported by Scott.[37] The fitted results over a wide range of E_0 confirmed the linear relationship too.

The scaling behavior as revealed presents us with a clear and simple physical picture with which the empirical relations, Eqs. (17) and (18), work indeed, at least for ferrite-based ferromagnetic solids and ferroelectric BTO and KNO. Although the experiments on various systems and by different researchers may show variation from one to another, the as-derived relationships are not very different from Eq. (14).

G. Remarks

The scaling behavior as revealed in the present model spin system relies on the assumption that the hysteresis is completely attributed to the spin-reversal mechanism, without contribution from any others. This assumption is questionable as f is extremely high where internal induction becomes serious with significant loss. Also, the dielectric effect should be taken into account too for realistic systems, especially for insulating magnetic solids. As for ferroelectric solids, the contribution over the extremely high frequency may be mainly from the electron or ion polarization, which is not considered here at all.

Although we demonstrate the scaling behavior for the present model system, no sufficient experimental evidence is available up to date. Also, a mathematical form of the scaling function $W(\eta)$ and its analytical dependence on temperature r and nonlinear correlation u have not yet been derived out. These issues seem not easy, considering the fact that the Langevin-type equation (4) has no analytical solution.

IV. CONCLUSION

In summary, we have presented a systematic calculation of the hysteresis dispersion in the model continuum spin systems based on the three-dimensional $(\Phi^2)^2$ model with $O(N)$ symmetry in the limit $N \to \infty$. The scaling behavior for the single-peak dispersion relation has been demonstrated for this model spin system once the amplitude of the external field is not very small. This scaling effect allows us to predict the existence of a characteristic time for the irreversible spin reversal that is responsible for the hysteresis generation, by which the hysteresis dispersion is uniquely predictable. The characteristic time shows an inversely linear dependence on the field amplitude, well consistent with the well-evidenced empirical relation for ferrites and ferroelectric solids.

ACKNOWLEDGMENTS

The authors acknowledge support from the Materials Research Centre of the Hong Kong Polytechnic University, the NSFC, and the National Key Projects for Basic Research of China as well as LSSMS of Nanjing University.

*Electronic address: liujm@nju.edu.cn

[1] G. Bertotti, *Hysteresis in Magnetism* (Academic, New York, 1998).
[2] J. D. Gunton, M. San Miguel, and P. S. Sahni, in *Phase Transitions and Critical Phenomena*, edited by C. Domb and J. L. Lebowitz (Academic, London, 1983), Vol. 8, p. 1.
[3] B. K. Chakrabarti and M. Acharyya, Rev. Mod. Phys. **71**, 847 (1999).
[4] G. Bate, J. Magn. Magn. Mater. **100**, 413 (1991).
[5] T. Tome and M. J. de Oliveira, Phys. Rev. A **41**, 4251 (1990).
[6] W. S. Lo and R. A. Pelcovits, Phys. Rev. A **42**, 7471 (1990).
[7] M. Acharyya, Phys. Rev. E **59**, 218 (1999).
[8] M. Acharyya and B. K. Chakrabarti, Phys. Rev. B **52**, 6550 (1995).
[9] M. Acharyya, J. K. Bhattacharjee, and B. K. Chakrabarti, Phys. Rev. E **55**, 2392 (1997).
[10] J. Smit and H. P. J. Wijn, *Ferrites* (Wiley, New York, 1959).
[11] M. Rao, H. R. Krishnamurthy, and R. Pandit, Phys. Rev. B **42**, 856 (1990).
[12] M. Rao and R. Pandit, Phys. Rev. B **43**, 3373 (1991).
[13] D. Dhar and P. B. Thomas, J. Phys. A **25**, 4967 (1992).
[14] P. B. Thomas and D. Dhar, J. Phys. A **26**, 3973 (1993).
[15] S. W. Sides, P. A. Rikvold, and M. A. Novotny, Phys. Rev. E **57**, 6512 (1998).
[16] P. A. Rikvold and B. M. Gorman, in *Annual Reviews of Computational Physics*, edited by D. Stauffer (World Scientific, Singapore, 1994), Vol. I, p. 149.
[17] M. Acharyya and D. Stauffer, Eur. Phys. J. B **5**, 571 (1998).
[18] P. Jung, G. Gray, R. Roy, and P. Mandel, Phys. Rev. Lett. **65**, 1873 (1990).
[19] C. N. Luse and A. Zangwill, Phys. Rev. E **50**, 224 (1994).
[20] A. Hohl, H. J. C. Linden, R. Roy, G. Goldsztein, F. Broner, and S. H. Strogatz, Phys. Rev. Lett. **74**, 2220 (1995).
[21] G. H. Goldsztein, F. A. Broner, and S. H. Strogatz, J. Appl. Math. Mech. **57**, 1163 (1997).

[22] G. P. Zheng and J. X. Zhang, J. Phys.: Condens. Matter **10**, 275 (1998).
[23] P. Bruno, G. Bayreuther, P. Beauvillain, C. Chappert, G. Luget, D. Renard, J. P. Renard, and J. Seiden, J. Appl. Phys. **68**, 5759 (1990).
[24] Q. Jiang, H. N. Yang, and G. C. Wang, Phys. Rev. B **52**, 14 911 (1995).
[25] Q. Jiang, H. N. Yang, and G. C. Wang, J. Appl. Phys. **79**, 5122 (1996).
[26] J. S. Suen and J. L. Erskine, Phys. Rev. Lett. **78**, 3567 (1997).
[27] J.-M. Liu, H. P. Li, C. K. Ong, and L. C. Lim, J. Appl. Phys. **86**, 5198 (1999).
[28] M. Acharyya and B. K. Chakrabarti, in *Annual Reviews of Computational Physics*, edited by D. Stauffer (World Scientific Publishers, Singapore, 1994), Vol. I, p. 107.
[29] H. Orihara, S. Hashimoto, and Y. Ishibashi, J. Phys. Soc. Jpn **63**, 1031 (1994).
[30] S. Hashimoto, H. Orihara, and Y. Ishibashi, J. Phys. Soc. Jpn **63**, 1610 (1994).
[31] H. Furukawa, Adv. Phys. **34**, 703 (1985).
[32] G. Mazenko and M. Zannetti, Phys. Rev. B **32**, 4565 (1985).
[33] A. Craevich and J. M. Sanchez, Phys. Rev. Lett. **18**, 1308 (1981).
[34] T. M. Rogers, K. R. Elder, and R. C. Desai, Phys. Rev. B **37**, 9638 (1988).
[35] T. Koma and H. Tasaky, Phys. Rev. Lett. **74**, 3916 (1995).
[36] H. L. Stadler and P. L. Zachmanids, J. Appl. Phys. **34**, 3255 (1963); **35**, 2895 (1964).
[37] J. F. Scott, Ferroelectr. Rev. **1**, 1 (1998).